Novel *exc* Genes Involved in Formation of the Tubular Excretory Canals of *C. elegans*

Hikmat Al-Hashimi*, Travis Chiarelli*,[1], Erik A. Lundquist*, and Matthew Buechner*

*Dept. of Molecular Biosciences, University of Kansas, Lawrence, KS, 66045, USA

[1]Present address: Dept. of Biological Sciences, University of Idaho, Moscow, ID, 83843, USA

Short Title:

RNAi Screen for Tubulogenesis Genes

Keywords

Tubulogenesis; lumen formation; endosomes; EXC-5; Charcot-Marie-Tooth Syndrome Type 4H

Corresponding Author:

Matthew Buechner

Dept. of Molecular Biosciences

1200 Sunnyside Avenue, 8035 Haworth Hall

University of Kansas

Lawrence, KS, 66045-7534

buechner@ku.edu

(785) 864-4328

ABSTRACT

Regulation of luminal diameter is critical to the function of small single-celled tubes, of which the seamless tubular excretory canals of *C. elegans* provide a tractable genetic model. Mutations in several sets of genes exhibit the Exc phenotype, in which canal luminal growth is visibly altered. Here, a focused reverse genomic screen of genes highly expressed in the canals found 24 genes that significantly affect luminal outgrowth or diameter. These genes encode novel proteins as well as highly conserved proteins involved in processes including gene expression, cytoskeletal regulation, vesicular movement, and transmembrane transport. In addition, two genes act as suppressors on a pathway of conserved genes whose products mediate vesicle movement from early to recycling endosomes. The results provide new tools for understanding the integration of cytoplasmic structure and physiology in forming and maintaining the narrow diameter of single-cell tubules.

INTRODUCTION

Tubule formation is an essential process during development of multicellular organisms, with the narrowest tubes occurring in structures as diverse as *Drosophila* trachea, floral pollen tubes, and mammalian capillaries (LUBARSKY and KRASNOW 2003; SIGURBJÖRNSDÓTTIR *et al.* 2014). In *C. elegans*, the excretory system is comprised of cells that form single-celled tubules of three types: pore cells that wrap around a lumen to form a tube with an autocellular junction ("seamed tube"); a larger duct cell that forms a similar tube followed by dissolution of the junction to form a "seamless" tube; and the large excretory canal cell that extends four long seamless tubules ("canals") throughout the length of the organism (SUNDARAM and BUECHNER 2016).

Many mutants have been discovered that affect the length, guidance of outgrowth, or lumen diameter of the excretory canals. An initial set of such identified "*exc*" mutants were mapped (BUECHNER *et al.* 1999), and found to include multiple alleles of some *exc* genes, but only single alleles of others. The frequency of mutations suggested that additional genes should have excretory lumen defects. Studies by multiple laboratories indeed found alleles of other genes with Exc phenotypes (KHAN *et al.* 2013; KOLOTUEV *et al.* 2013; ARMENTI *et al.* 2014; LANT *et al.* 2015; GILL *et al.* 2016; FORMAN-RUBINSKY *et al.* 2017). Almost all of the original *exc* genes have now been cloned (SUZUKI *et al.* 2001; BERRY *et al.* 2003; FUJITA *et al.* 2003; PRAITIS *et al.* 2005; TONG and BUECHNER 2008; MATTINGLY and BUECHNER 2011; SHAYE and GREENWALD 2015; GRUSSENDORF *et al.* 2016; AL-HASHIMI *et al.* 2018), and found to affect multiple well-conserved cell processes, including cytoskeletal structures, ion channels, and vesicle recycling pathways. The initial screen sought primarily non-lethal genetic effects, but several of the subsequently identified genes were lethal when null.

RNAi studies have been particularly useful in determining roles of excretory canal genes where the null allele is lethal, such as the gene encoding the NHR-31 nuclear hormone receptor (HAHN-WINDGASSEN and VAN GILST 2009), the ABI-1 Abelson-Interactor (MCSHEA *et al.* 2013), and the PROS-1 transcription factor (KOLOTUEV *et al.* 2013). In addition, null mutations in genes that connect the excretory canal cell to the excretory duct (e.g. LET-4 (MANCUSO *et al.* 2012) and LPR-1 (FORMAN-RUBINSKY *et al.* 2017)) are lethal.

In order to identify other genes affecting the process of tubulogenesis and tubule maintenance in the excretory canals, we undertook a targeted genomic RNAi screen to identify excretory canal genes that exhibit lumen alterations ("Exc" phenotypes) when knocked down. This screen confirmed or identified 24 genes preferentially expressed in the canals that showed effects on lumen and/or outgrowth of the excretory canals, including 17 genes with no prior known phenotypic effects on the canals. In addition, two knockdowns suppressed effects of mutation of the *exc-5* vesicle-recycling gene, and therefore represent potential regulators of vesicle transport needed for single-cell tubulogenesis.

77 # MATERIALS AND METHODS

78 **Nematode genetics:**

79 *C. elegans* strains (Table 1) were grown by use of standard culture techniques on lawns
80 of *Escherichia coli* strain BK16 (a streptomycin-resistant derivative of strain OP50) on nematode
81 growth medium (NGM) plates (SULSTON and HODGKIN 1988). All strains were grown and
82 evaluated for canal phenotypes at 20°C. Worms observed in this study were young adults or
83 adults.

84 Each nematode strain (wild-type N2, and *exc-2*, *exc-3*, *exc-4*, *exc-5*, *and exc-7*) was
85 crossed to strain BK36, which harbors a chromosomal insertion of a canal-specific promoter
86 driving cytoplasmic GFP expression ($P_{vha\text{-}1}$*::gfp*). Strains were then sensitized for RNAi
87 treatment by crossing them to mutant strain BK540 (a strain carrying *rrf-3*(*pk1426*) in addition to
88 the same chromosomal *gfp* insertion as above) and selecting in the F2 generation for
89 homozygous *rrf-3* deletion allele and appropriate *exc* mutation. (As *exc-7* maps very close to *rrf-*
90 *3*, the *exc-7* strain carrying *gfp* was not crossed to BK540 and was not sensitized to RNAi). For
91 all sensitized strains, the *rrf-3* deletion was confirmed via PCR using the forward primer
92 $^{5'}$TGCTTTGGATATTGCCGAGCAC$^{3'}$, reverse primer $^{5'}$GGAGATCTCCGAGCCCTAGAC$^{3'}$,
93 and a reverse nested primer $^{5'}$CATCGCCAGGCCAACTCAATAC$^{3'}$. As a negative control, we
94 crossed BK36 to RNAi-refractive strain NL3321 *sid-1*(*pk3321*).

95 **RNAi Screen:**

96 The Ahringer RNAi bacterial library (KAMATH *et al.* 2003) was utilized for this study.
97 Overnight cultures were prepared by inoculating bacteria in 5 ml LB + ampicillin (100µg/ml) +
98 tetracycline (12.5µg/ml), and cultured at 37°C for 16 hours. In order to induce the bacteria with
99 IPTG, overnight cultures were moved to fresh media, incubated at 37°C with rotation until
100 cultures reached an $O.D._{600}$ in a range from 0.5 to 0.8. IPTG was then added to the culture to a

final concentration of 95 µg/ml along with ampicillin at 100µg/ml. The cultures were then incubated with rotation at 37ºC for ninety minutes followed by re-induction with IPTG and ampicillin, and another ninety minutes of incubation at 37ºC with rotation. Finally, IPTG and ampicillin were added for the last time right before using these bacteria to seed NGM in 12-well plates and Petri dishes. Plates were then incubated at room temperature for 24 hours in order to dry. L2 worms were added to the plates, and their F1 progeny were evaluated for phenotypes in the excretory canals. Each set of genes tested was induced together with induction of the *sid-1* negative control strain BK541 and of two positive control strains: a plate of bacteria induced to knock down *dpy-11* (which affects the hypoderm but not the canals) (BRENNER 1974), and a plate of bacteria induced to knock down *erm-1* bacteria, which causes severe defects in excretory canal length and lumen diameter (KHAN *et al.* 2013), respectively. Induction was considered successful and plates were screened only if worms grown on the control plates showed the appropriate phenotypes in at least 80% of the surviving progeny.

For each tested gene, the induced bacteria were seeded on one 12-well plate and one 60mm plate. Two or three L2 nematodes were placed on the bacterial lawn of each well, and screened for phenotypes in the 4th, 5th, and 6th days of induction. Each gene was tested via RNAi treatment of twelve different strains of worms, shown in Table 1, while the sole 60mm plate was used for further analysis of animals with wild-type canals (strain BK540, Table 1) grown on the RNAi-expressing bacteria. For assessment of a canal effect, a minimum of five animals showing a canal phenotype were collected, examined, and in most cases photographed; for most genes, 10-20 affected animals were examined closely. For the 24 genes showing effects, the entire experiment was subsequently repeated, with induction and growth of bacteria solely on 60mm plates and feeding tested on BK540 (RNAi-sensitized wild-type with integrated canal marker) worms.

Microscopy:

Living worms were mounted on 3% agarose pads to which were added 0.1µm-diameter Polybead® polystyrene beads (Polysciences, Warrington, PA) to immobilize the animals (KIM *et al.* 2013). Images were captured with a MagnaFire Camera (Optronics) on a Zeiss Axioskop microscope equipped with Nomarski optics and fluorescence set to 488 nm excitation and 520 nm emission. Adobe Photoshop software was used to combine images from multiple sections of individual worms and to crop them. Contrast on images was uniformly increased to show the excretory canal tissue more clearly.

Canal Measurements:

For measuring effects of suppression of the Exc-5 phenotype, excretory canal length and cystic and suppression phenotypes were measured and analyzed as described (TONG and BUECHNER 2008). Canal length was scored by eye on a scale from 0-4: A score of (4) was given if the canals had grown out to full length; canals that extended halfway past the vulva (midbody) to full-length were scored as (3); at the vulva (2); canals that ended halfway between the cell body and the vulva were scored as (1); and if the canal did not extend past the cell body, the canal was scored as (0). For statistical analyses, canals were binned into three categories for length (scores 0-1, scores 1.5-3.0, and score 3.5-4), and the results then analyzed via a 3x2 Fisher's Exact Test (www.vassarstats.net).

Reagent and Data Availability:

All nematode strains used in this study are listed in Table 1. Bacterial clone numbers tested, and summary of test results are presented in Tables S1 and S2, available on Figshare. Gene names *exc-10* through *exc-18* and *suex-1* and *suex-2* have been registered with Wormbase (www.wormbase.org). Sensitized *exc* mutant strains are available upon request, and may be made available through the Caenorhabditis Genetics Center (CGC), University of Minnesota (cgc.umn.edu), pending acceptance to that repository. Other strains are available upon request.

RESULTS AND DISCUSSION

A focused RNAi screen for new *exc* mutations

A study of genomic expression in *C. elegans* was previously undertaken by the Miller lab (SPENCER *et al.* 2011). In that study, lists of genes highly expressed in various tissues, including 250 genes preferentially expressed in the excretory canal cell, were made public on the website WormViz (http://www.vanderbilt.edu/wormdoc/wormmap/WormViz.html). Of the corresponding strains in the Ahringer library of bacteria expressing dsRNA to specific *C. elegans* genes (KAMATH *et al.* 2003), we found that 216 grew well, and were tested for effects on the various *C. elegans* strains (Table S1).

The excretory canal cell has some characteristics similar to those of neurons: long processes guided by netrins and other neural guidance cues (HEDGECOCK *et al.* 1987), as well as early expression of the gene EXC-7/HuR/ELAV (FUJITA *et al.* 2003), and so was considered potentially refractory to feeding RNAi (CALIXTO *et al.* 2010). We crossed strain BK36, containing a strong canal-specific integrated *gfp* marker, to a mutant in the *rrf-3* gene (*pk1426*) in order to increase sensitivity to RNAi (SIMMER *et al.* 2002) to create strain BK540. In addition, we also crossed the same *gfp* marker and *rrf-3* mutation to excretory canal mutants *exc-2*, *exc-3*, *exc-4*, *exc-5*, and *exc-7* (except that *exc-7* was not RNAi-sensitized; see Materials and Methods). This was done in order to determine if the tested gene knockdowns interacted with known *exc* genes affecting excretory canal tubulogenesis, since double mutants in some *exc* genes (e.g. *exc-3*; *exc-7* double mutants (BUECHNER *et al.* 1999)) exhibit more severe canal phenotypes than either mutant alone.

We demonstrated the effectiveness of the treatment by performing successful

knockdowns of canal-specific and –non-specific genes in these strains. Control knockdowns of *dpy-11* resulted in short worms with normal canal phenotypes, while knockdown of *exc-1* caused formation of variable-sized cysts in a shortened excretory canal, with no other obvious phenotypes (Fig. 1). Here, knockdown of the ezrin-moesin-radixin homologue gene *erm-1* (GÖBEL *et al.* 2004; KHAN *et al.* 2013) caused severe malformation of the canals visible in 80% of surviving treated worms. A deletion mutant of this gene is often lethal due to cystic malformation of the intestine as well as the canals (GÖBEL *et al.* 2004), while our treatment allowed many animals to survive to adulthood and reproduce. This result is consistent with our RNAi treatment causing variable levels of gene knockdown (TIMMONS AND FIRE 1998) in the excretory canals.

Of the 212 non-control genes tested, 182 caused no obvious phenotypic changes to the canals of BK540 worms, and 4 gave very low numbers (less than 5) of animals with mild defects. Knockdown of 24 genes caused noticeable defects in the development of the excretory canals in at least 5-10 worms, and gave this result upon retesting of these strains (Table 2, Table S2). The length of the canals was rated according to a measure shown in Fig. 1A, in which no extension past the excretory cell body was rated 0, extension to the animal midbody marked by the position of the vulva was measured as 2, and full extension was rated as 4. The average canal length of affected animals was characteristic for the gene knocked down (Table 2), although RNAi knockdown via feeding is intrinsically variable in the strength of gene induction and amount of bacteria eaten, so the observed canal length is likely longer than if the gene were fully and uniformly knocked out. Diameter of the canals also varied greatly, depending on the gene knocked down; in cases where fluid-filled cysts became evident (as in previously-described *exc* mutants), cyst size was rated as large (cyst diameter at least half the width of the animal), medium (one-quarter to one-half animal width), or small (up to one-quarter animal width).

198 Finally, use of feeding RNAi knockdown allowed observation of gene effects where knockouts
199 have been reported to be lethal.

200 **Excretory Canal Phenotypes**

201 The common feature of all of these knockdown animals is that the posterior canals did
202 not extend fully to the back of the animal (Table 2). The length of the canal lumen was often the
203 same as the length of the canal cytoplasm, but in many cases the visible lumen (seen as a dark
204 area in the center of the GFP-labelled cytoplasm) was substantially shorter than the length of the
205 canal cytoplasm.

206 In addition to effects on canal length, the shape and width of the canal lumen and/or canal
207 cytoplasm was affected by specific gene knockdown: A) Several knockdowns resulted in the
208 formation of fluid-filled cysts reminiscent of those in known *exc* mutants; B) Canals appeared
209 normal in diameter, but had frequent thickenings of cytoplasm around otherwise normal (but
210 short) lumen similar to the 'beads" or "pearls" seen in growing first-larval-stage canals or in
211 canals of animals undergoing osmotic stress (KOLOTUEV *et al.* 2013); C) Canal lumen ending in
212 a large swelling of convoluted tubule or a multitude of small vesicles, and often with a "tail" of
213 very thin canal cytoplasm without any lumen continuing distally; D) a series of vesicles filling
214 much of the cytoplasm outside the normal-diameter lumen, and; E) an irregular shape of the
215 basal surface of the cytoplasm, varying widely in diameter. Each of these phenotypes will be
216 discussed below, together with the genes whose knockdown resulted in that phenotype.

217 CYSTIC CANALS: Two gene knockdowns, of *ceh-6* and of T25C8.1 (which will be
218 referred to as *exc-10*) resulted in the formation of large fluid-filled cysts (Fig. 2), similar to those
219 seen in *exc-2*, *exc-4*, and *exc-9* mutants (encoding an intermediate filament, a CLC chloride
220 channel, and a CRIP vesicle-trafficking protein, respectively (TONG and BUECHNER 2008;

221 BERRY *et al.* 2003, Al-Hashimi, in press). The homeobox gene *ceh-6* encodes a well-studied
222 transcription factor that defines expression of many genes in the canal (BURGLIN and RUVKUN
223 2001; ARMSTRONG and CHAMBERLIN 2010). Null mutants of this gene are lethal. The
224 knockdowns had very short canals with large fluid-filled cysts. The effect of *ceh-6* knockdown
225 could reflect lower transcription of many of the known *exc* genes, effects on the excretory
226 aquaporin *aqp-8* (MAH *et al.* 2007), or of a novel gene.

227 The second gene, T25C8.1 (*exc-10*) encodes a carbohydrate kinase (homology to
228 sedoheptulose kinase) of unknown function in nematodes, although the human homologue SHPK
229 has been linked to a lysosomal storage disease (PHORNPHUTKUL *et al.* 2001; WAMELINK *et al.*
230 2008).

231 Knockdowns in *mop-25.2*, *egal-1*, F41E7.1 (*exc-11*), and T05D4.3 (*exc-12*) exhibited
232 small-to-medium sized cysts (Fig. 2). In these animals, cystic regions of the lumen often appear
233 to contain a series of hollow spheres, which may be connected or separate from each other along
234 the lumen length (Fig. 2C-F). The EGAL-1 protein is a homologue of the *Drosophila*
235 Egalitarian exonuclease involved in RNA degradation. EGAL-1 also interacts with dynein as
236 part of a dynein-regulating complex at the face of the nucleus (FRIDOLFSSON *et al.* 2010) and
237 regulates polarity of the *Drosophila* egg chamber through organization of oocyte microtubules
238 (SANGHAVI *et al.* 2016). The excretory canal cell is rich in microtubules along the length of the
239 canals (BUECHNER *et al.* 1999; SHAYE and GREENWALD 2015).

240 MOP-25.2 is a protein with close homology to yeast Mo25 and its homologues in all
241 animals, and acts as a scaffolding protein for activating kinases including germinal center kinase
242 at the STRIPAK complex, which also regulates RAB-11-mediated endocytic recycling in the
243 excretory canal morphology and gonadal lumen formation in *C. elegans* (LANT *et al.* 2015; PAL

et al. 2017). The *Drosophila* Mo25 also regulates transepithelial ion flux in the osmoregulatory Malpighian tubules (SUN *et al.* 2018).

F41E7.1 (*exc-11*) encodes a solute carrier with high homology to the Na^+/H^+ exchanger. The excretory cell lumen is associated with small canaliculi that have high levels of the vacuolar ATPase to pump protons into the canal lumen (OKA *et al.* 2001), so the presence of a Na^+/H^+ exchanger could be used for canal osmoregulatory function as well as luminal shape.

Finally, T05D4.3 (*exc-12*) is homologous only to genes in other nematodes, and has no obvious function, other than the presence of several putative transmembrane domains.

PERIODIC CYTOPLASMIC SWELLINGS: These "beads" or "pearls" are commonly seen in wild-type animals with growing canals at the L1 stage and in animals under osmotic stress (KOLOTUEV *et al.* 2013). These sites are hypothesized to be locations of addition of membrane to allow the canal to continue to grow together with the animal. The knockdown animals here were measured in young adulthood, and so should not exhibit such beads. Knockdown of the *inx-12* or *inx-13* genes (Fig. 3), which encode innexins highly expressed in the canals (and in the adjacent CAN neurons), gave rise to these structures. Innexins form the gap junctions of invertebrates (HALL 2017), and the excretory canals are rich in these proteins along the basal surface, where they connect the canal cytoplasm to the overlaying hypodermis (NELSON *et al.* 1983). Null mutants in either of these two genes results in early larval rod-like swollen lethality consistent with excretory cell malfunction (ALTUN *et al.* 2009). The knockdown phenotype here further suggests that these proteins regulate balancing of ionic content to allow normal canal growth.

A similar phenotype is seen in animals knocked down for *ceh-37*, which encodes a well-conserved Otx Homeobox protein expressed solely in the excretory cell in adults, but

267 additionally in a wide range of tissues in embryos (LANJUIN *et al.* 2003; HENCH *et al.* 2015), and
268 which binds preferentially to telomeric DNA (MOON *et al.* 2014). Expression of *ceh-37* is itself
269 regulated by CEH-6 (BURGLIN and RUVKUN 2001), so the difference in phenotypes of
270 knockdowns of these two genes suggests that CEH-6 regulates a wider range of genes than does
271 CEH-37.

272 Knockdown of *dhhc-2* shows a similar phenotype, although bead size and placement
273 appears more irregular than for the above knockdowns (Fig. 3). Close examination of the beads
274 shows numerous small dark spots consistent with the presence of many vesicles of varying sizes
275 within the beads (Fig. 3D) This gene encodes a zinc-finger protein homologous orthologous to
276 human ZDHHC18, which acts as a protein palmitoyltransferase, possibly for small GTPase
277 proteins (OHNO *et al.* 2012). A previous knockdown study of this gene (EDMONDS AND MORGAN
278 2014) showed no obvious effects on morphology or behaviour, although combined knockdown
279 of both *dhhc-2* together with its close homologue *dhhc-8* resulted in reduced lifespan for
280 unknown reasons.

281 Finally, the "bead" phenotype is also seen in knockdown of *mxt-1*, an RNA-binding
282 protein that binds to eukaryotic initiation factor 4E to regulate translation rates (PETER *et al.*
283 2015) (Fig. 3E).

284 SWELLING AT END OF LUMEN: The largest group of knockdown animals showed a
285 substantial swelling at the distal tip of generally normal-diameter canals (Fig. 4). In some cases,
286 the swelling appears to be caused by accumulation of a convoluted lumen folded back on itself,
287 while in other knockdowns this swelling could reflect accumulation of a large number of vesicles
288 at the end of the lumen. A combination of these structures also appears in many animals.
289 Reflecting the variable effects of RNAi knockdown, some animals knocked down in genes

290 discussed above, *ceh-37* and *mop25.2*, sometimes showed a highly convoluted lumen primarily
291 at the distal tip (Fig. 4C, 4H), possibly reflecting weaker knockdown than in other examples
292 where the entire lumen was affected. Knockdown of another gene, *best-3*, showed a similar
293 effect (Fig. 4G). This gene encodes one of a large family of chloride channels homologous to
294 human bestrophins, chloride channels found in muscle, neurons, and the eye, that are essential
295 for Ca^{++} signaling, and defective in retinal diseases (STRAUSS *et al.* 2014).

296 Knockdowns of *gst-28* and of *fbxa-183* (Fig. 4A, 4D) show clear and dramatic
297 accumulation of vesicles at the swelling at the tip of the lumen. Vesicle transport defects are the
298 cause of canal malformations in *exc-1*, *exc-5*, and *exc-9* mutants (TONG and BUECHNER 2008;
299 MATTINGLY and BUECHNER 2011; GRUSSENDORF *et al.* 2016), so the knockdown effects shown
300 in these and the following genes may reflect similar defects in vesicular transport. GST-28 is a
301 glutathione-S-transferase orthologous to the human prostaglandin D synthase, which isomerizes
302 PGH_2 to form prostaglandin (CHANG *et al.* 1987). FBXA-183 is one of the very large family of
303 F-box proteins in *C. elegans* that facilitate targeting substrates for E3 ubiquitinase-mediated
304 destruction (KIPREOS AND PAGANO 2000). FBXA-183 also contains an FTH (FOG-2 Homology)
305 domain; in FOG-2, this domain binds GLD-1, an RNA-binding protein (CLIFFORD *et al.* 2000).

306 Knockdown of three genes produced animals with swollen distal canal tips filled with a
307 mixture of convoluted tubule and individual vesicles. The *gsr-1* gene (Fig. 4B) encodes the sole
308 glutathione reductase in *C. elegans*, necessary for rapid growth and embryonic development as
309 well as canal morphology (MORA-LORCA *et al.* 2016). T19D12.9 (to be referred to as *exc-13*)
310 (Fig. 4E) encodes another homologue of the human SLC family of solute carriers, including the
311 ubiquitous lysosomal membrane sialic acid transport protein sialin (SLC17A5), which transports
312 sialic acid from the lysosome, and nitrate from the plasma membrane in humans (QIN *et al.*
313 2012). C09F12.3 (to be referred to as *exc-18*) encodes a protein found predominantly in

nematodes and likely encoding a 7-tm G-Protein-Coupled Receptor of the FMRFamide class, used to respond to the wide range of FMRFamide-Like Peptides (FLP) mediating multiple behaviors in invertebrates (PEYMEN *et al.* 2014). Finally, knockdown of the germinal center kinase gene *gck-3* (Fig. 4I) caused this phenotype. As noted above, germinal center kinase acts at the STRIPAK complex to regulate maintain canal morphology, and malformations affecting STRIPAK cause tubule defects such as cavernous cerebral malformations in humans (LANT *et al.* 2015).

A very narrow canal "tail" completely lacking a visible lumen often extends substantially past the end of the lumenated portion of the canal in these animals (Fig. 4B, 4C, 4G, 4I). This tail follows the path of wild-type canal growth, and in a few rare instances even reaches the normal endpoint of the canal. In wild-type animals, the lumen and tip of the canal grow together and reach the same endpoint (BUECHNER *et al.* 1999), with a widening suggestive of a growth cone at the tip of the growing canal in the embryo and L1 stage (FUJITA *et al.* 2003). The tip of the canal is enriched in the formin EXC-6, which mediates interactions between microtubules and actin filaments and may mediate connections between the canal tip and end of the lumen (SHAYE and GREENWALD 2015). The results here are consistent with the idea that canal lumens grow and extend separately from the growing basal surface that guides cytoplasmic outgrowth (KOLOTUEV *et al.* 2013).

A NOVEL EXCRETORY PHENOTYPE: VESICLES ALONG LENGTH OF SWOLLEN CANAL CYTOPLASM: Knockdown of some genes gave rise to a phenotype that has not, to our knowledge, been observed before within the excretory canals (Fig. 5). Knockdown of the gene K11D12.9 (which will be referred to as *exc-14*) exhibited an extraordinary increase of vesicles in the cytoplasm of the canal, terminating in a large irregular swelling at the end of the canal (Fig. 5A, 5A'). This swelling is unusual in that the lumen of the

canal appears relatively normal in diameter (though short), but is surrounded by cytoplasm that puffs out at the basal side of the cell, which is surrounded by (and extensively connected via innexins to) the hypoderm and by basement membrane abutting the pseudocoelom (NELSON *et al.* 1983). GFP labelling of the cytoplasm showed the thick layer of canaliculi surrounding the lumen, which is surrounded by a cytoplasm packed with vesicles of variable size. K11D12.9 encodes a protein containing a RING finger domain at the C-terminus, with BLASTP homology to potential ubiquitin E3-ligases found in plants and animals.

Knockdown of several other genes gave rise to vesicles of varying size in the cytoplasm plus irregular swellings to the side of the canal, some primarily at the terminus of the lumen, and in some cases along the length of the canals (Fig. 5B-5F). These included some animals knocked down in the F-Box gene *fbxa-183*, discussed above. Knockdowns of T08H10.1 (which will be referred to as *exc-15*) or of H09G03.1 (*exc-16*) showed increasing amounts of variable-sized vesicles in the canal cytoplasm towards the distal ends of the canals, together with increasing numbers of irregular cysts in the lumen (Fig. 5C, 5D). H09G03.1 has no conserved domains, and no clear homology to genes outside the *Caenorhabditis* genus. T08H10.1, however, encodes a well-conserved aldo-keto-reductase (family 1 member B10), and in a previous RNAi screen knockdowns of this gene slowed the defecation rate by about 20%, possibly through effects on mitochondrial stress (LIU *et al.* 2012).

Knockdown of two other genes caused the appearance of large cysts or vesicles appearing on the basal surface of the canals in just a few seemingly random spots along the length of the canals (Fig. 5E, 5F). C03G6.5 (*exc-17*) encodes another protein found only in nematodes, with a Domain of Unknown Function (DUF19), possibly an extracellular domain, found only among several nematode and bacterial proteins. CYK-1, however, is a formin of the Diaphanous class, that has a well-investigated role in regulating microfilaments in cytokinesis

(SEVERSON *et al.* 2002), and in forming normal canal morphology through interactions with the EXC-6 formin, via regulation by EXC-5 (human FGD) guanine exchange factor and CDC-42 (SHAYE and GREENWALD 2016). Our RNAi knockdown of *cyk-1* produced a stronger phenotype (shorter canals with large cysts on the basal side) than seen in the temperature-sensitive mutant used by the Greenwald laboratory, but not as strong an effect as was seen in double mutants of *cyk-1*(*ts*) with *exc-6* null mutants (SHAYE and GREENWALD 2016).

Variability and Range of Phenotypes:

Treatment of nematodes via feeding RNAi creates variable levels of knockdown between animals (HULL and TIMMONS 2004). This feature of the gene knockdowns has allowed observation of effects of genes that have a lethal null phenotype, and show a relationship between the phenotypes described above, as seen from RNAi-knockdown of the *vha-5* gene. This gene encodes a protein of the membrane-bound V0 subunit of the vacuolar ATPase, and is strongly expressed in the canalicular vesicles at the apical membrane of the canals (KOLOTUEV *et al.* 2013). Mutations of this gene are lethal, and a point mutation led to strong whorls of labelled VHA-5 at the apical surface (LIEGEOIS *et al.* 2006). Our knockdown of this gene gave a wide range of canal phenotypes in different animals (Fig. 6). Some animals exhibited beads surrounding a normal-diameter lumen (Fig.6A), similar to animals under slow growth or osmotic stress, as in Fig. 3. Other animals showed small septate cysts in the canal lumen, but the canal lumen overall was generally of near-normal diameter, and the basal surface had mostly minor irregularities (Fig. 6B), similar to animals knocked down for *exc-15* (Fig. 5D). Other *vha-5* knockdown animals also exhibited a similar luminal phenotype, but also showed large vesicles within a highly irregularly shaped cytoplasm (Fig. 6C), similar to animals impaired in *exc-17* or *cyk-1* expression (Fig. 5E, 5F). Finally, the most extremely affected *vha-5* knockdown animals (Fig. 6D) showed cysts throughout the lumen, a swollen terminus to the lumen, and a range of

386 variable-sized vesicles or cysts that pack the entire swollen cytoplasm of the canals. The wide
387 range of defects seen in animals knocked down may reflect the very strong phenotype of the null
388 mutant (embryonic lethal), and the wide range of expression of dsRNA that can occur through
389 feeding RNAi. The variability of phenotype also indicates that the range of mutant phenotypes
390 described above for various gene knockdowns may represent variable expression of dsRNAs that
391 affect a common set of coordinated pathways that function to create and maintain the
392 complicated shape of the excretory canals; these pathways include gene transcription, ion and
393 small molecule transport, cell cytoskeleton, cell-cell communication, and movement and
394 function of vesicles.

395 **Other Phenotypes**

396 While the focus of this RNAi screen centered on excretory canal morphology, a few other
397 phenotypes were noticed, including occasional effects on gonadal shape, fertility, and viability.
398 In many *exc* mutants, the shape of the hermaphrodite tail spike is affected (BUECHNER *et al.*
399 1999), and similar strong results were reproducibly observed here for multiple RNAi
400 knockdowns (Fig. 7). In addition to the knockdowns shown (for genes *exc-11*, *exc-14*, *egal-1*,
401 *mop-25.2*, and *inx-12*), tail spike defects were also seen in animals knocked down in genes
402 encoding homeobox protein CEH-6, vacuolar ATPase component VHA-5, sedoheptulose kinase
403 EXC-10, aldo-keto reductase EXC-15, and innexin INX-13. The tail spike is formed from the
404 interaction of hypodermal tissue hyp10 with a syncytium of two other hypodermal cells that later
405 undergo cell death (SULSTON *et al.* 1983); it remains to be determined what features this
406 structure has in common with the canals that require the same proteins.

407 **Suppressors of the Exc-5 Phenotype**

408 Finally, the RNAi screen was also carried out in animals carrying mutations in various

409 *exc* genes, to try to find genes that interacted to form more severe phenotypes. Previous
410 interactions have found, for example, that *exc-3*; *exc-7* double mutants have a more severe canal
411 phenotype than does either mutant alone (BUECHNER *et al.* 1999), and similar exacerbation of
412 effects are seen for *exc-5*; *exc-6* double mutants (LIEGEOIS *et al.* 2006). No such effects were
413 detected in this screen, but surprisingly, knockdown of two genes caused an unexpected
414 phenotype: the restoration of near-wild-type phenotype from strongly cystic homozygous *exc-*
415 *5*(*rh232*) animals (Fig. 8) carrying a large deletion of almost all of the *exc-5* gene (SUZUKI *et al.*
416 2001). As noted above, *exc-5* encodes a Guanine Exchange Factor (GEF) specific for CDC-42
417 (SHAYE and GREENWALD 2016). EXC-5 is homologous to four human FGD proteins, including
418 two that are implicated in Aarskog-Scott Syndrome (Facio-Genital Dysplasia) and Charcot-
419 Tooth-Marie Syndrome Type 4H, respectively (GAO *et al.* 2001; DELAGUE *et al.* 2007; HORN *et*
420 *al.* 2012). The latter disease affects outgrowth of the single-celled tubular Schwann cells during
421 rapid growth, and identification of mutations in suppressor genes therefore has the potential to
422 increase understanding of this disease.

423 *exc-5* null mutants are characterized by large fluid-filled cysts at the terminus of both
424 anterior and posterior canals (Fig. 8). Knockdown RNAi of these suppressor genes, both by
425 feeding and by direct dsRNA microinjection, yielded a large number of progeny exhibiting near-
426 normal canal phenotypes, with canal length extending near-full-length (Fig. 8D). We will refer
427 to this phenotype as Suex, for SUppressor of EXcretory defects. In SUEX canals, no obvious
428 septate cysts are evident, although parts of the canal lumen were slightly widened (Fig. 8B, 8C).

429 F12A10.7 (*suex-1*) encodes a small protein (113 amino acids) unique to *C. elegans*,
430 expressed in the excretory canal cell and in some neural subtypes, with homology to genes in
431 only a few other *Caenorhabditis* species. The C-terminal half of the protein contains a number
432 of repeats of tri- and tetra-peptides GGY and GGGY. As the bacterial construct from the

433 Ahringer Library also included a small number of base pairs of the nearby gene F12A10.1, we
434 confirmed the identity of the suppressing gene through microinjection of synthesized dsRNA
435 specific to the F12A10.7 transcript into the gonad of the *exc-5* null mutant strain BK545, and
436 confirmed the appearance of progeny with canals of wild-type length.

437 In contrast to F12A10.7, C53B4.1 (*suex-2*) encodes a protein with homologues in a wide
438 range of animals, including humans. This gene encodes a cation transporter that has been
439 implicated in gonadal distal tip cell migration in a previous RNAi screen (CRAM *et al.* 2006).
440 Multiple strong homologues in humans fall into the SLC (SoLute Carrier) family 22 class of
441 proteins, with the closest homologue SLC22A1 encoding a 12-tm-domain integral membrane
442 protein transporting organic cations (NIGAM 2018) and expressed in the human liver and small
443 intestine. The effect of knocking down this transporter implies that ionic milieu or lipid
444 composition affects transport of vesicles mediated by EXC-5 signaling, but future work will be
445 needed to determine the role that this transporter exerts on ionic content, and possibly on
446 endosomal recycling in the developing excretory canal cell.

447

448 **CONCLUSION**

449 This RNAi screen was successful at identifying 24 genes (17 not implicated before) needed to
450 form a normal lumen of the long excretory canals of *C. elegans*. These genes encode
451 transcription and translation factors, innexins and other channels, and proteins involved in
452 trafficking, among others. While these processes have been implicated previously in canal
453 tubulogenesis, these proteins identify new actors that could provide insights into how these
454 cellular processes are integrated in single-cell tubulogenesis. Several other proteins have roles in
455 sugar metabolism and redox, which are new processes to be involved in canal morphogenesis.
456 Finally, two genes were identified as suppressors of *exc-5* mutation; determining the function of
457 these suppressor proteins has the potential to increase understanding of the function of FGD
458 protein function in normal development and in disease.

459

ACKNOWLEDGMENTS

H.A. was supported in part by KU Graduate Research Funds #2301847 and #2144091. E.A.L. was supported by National Institutes of Health grants #NS0090945, NS0095682, NS0076063, and GM103638. Some strains were provided by the CGC, which is funded by the NIH Office of Research Infrastructure Programs (P40 OD010440). RNAi-refractive strain NL3321 *sid-1*(*pk3321*) was the gift of Lisa Timmons, U. Kansas. Some strains were created by the *C. elegans* Reverse Genetics Core Facility at the University of British Columbia, which is part of the international *C. elegans* Gene Knockout Consortium.

AUTHOR CONTRIBUTIONS

M.B. and H.A. designed the research, with support from E.A.L. on strategies for RNAi treatments; H.A. and T.C. performed bacterial and nematode growth, performed RNAi treatments, and evaluation of canal phenotypes. E.A.L. supplied bacterial RNAi clones. M.B. and H.A. prepared the figures and wrote the manuscript.

LITERATURE CITED

AL-HASHIMI, H., D. H. HALL, B. D. ACKLEY, E. A. LUNDQUIST, and M. BUECHNER, 2018 Intermediate filaments EXC-2 and IFA-4 Maintain Luminal Structure of the Tubular Excretory Canals in Caenorhabditis elegans. Genetics, in press. https://doi.org/10.1534/genetics.118.301078

ALTUN, Z. F., B. CHEN, Z. W. WANG and D. H. HALL, 2009 High resolution map of Caenorhabditis elegans gap junction proteins. Dev Dyn **238:** 1936-1950. https://doi.org/10.1002/dvdy.22025

ARMENTI, S. T., E. CHAN and J. NANCE, 2014 Polarized exocyst-mediated vesicle fusion directs intracellular lumenogenesis within the C. elegans excretory cell. Dev Biol **394:** 110-121. https://doi.org/10.1016/j.ydbio.2014.07.019

ARMSTRONG, K. R., and H. M. CHAMBERLIN, 2010 Coordinate regulation of gene expression in the C. elegans excretory cell by the POU domain protein CEH-6. Mol Genet Genomics **283:** 73-87. https://doi.org/10.1007/s00438-009-0497-8

BERRY, K. L., H. E. BULOW, D. H. HALL and O. HOBERT, 2003 A C. elegans CLIC-like protein required for intracellular tube formation and maintenance. Science **302:** 2134-2137. https://doi.org/10.1126/science.1087667

BRENNER, S., 1974 The genetics of Caenorhabditis elegans. Genetics **77:** 71-94.

BUECHNER, M., D. H. HALL, H. BHATT and E. M. HEDGECOCK, 1999 Cystic Canal Mutants in *Caenorhabditis elegans* Are Defective in the Apical Membrane Domain of the Renal (Excretory) Cell. Developmental Biology **214:** 227-241. https://doi.org/10.1006/dbio.1999.9398

BURGLIN, T. R., and G. RUVKUN, 2001 Regulation of ectodermal and excretory function by the C. elegans POU homeobox gene ceh-6. Development **128:** 779-790.

CALIXTO, A., D. CHELUR, I. TOPALIDOU, X. CHEN and M. CHALFIE, 2010 Enhanced neuronal RNAi in C. elegans using SID-1. Nat Methods **7:** 554-559. https://doi.org/10.1038/nmeth.1463

CHANG, M., Y. HONG, J. R. BURGESS, C. P. TU and C. C. REDDY, 1987 Isozyme specificity of rat liver glutathione S-transferases in the formation of PGF2 alpha and PGE2 from PGH2. Arch Biochem Biophys **259:** 548-557.

CLIFFORD, R., M. H. LEE, S. NAYAK, M. OHMACHI, F. GIORGINI *et al.*, 2000 FOG-2, a novel F-box containing protein, associates with the GLD-1 RNA binding protein and directs male sex determination in the C. elegans hermaphrodite germline. Development **127:** 5265-5276.

CRAM, E. J., H. SHANG and J. E. SCHWARZBAUER, 2006 A systematic RNA interference screen reveals a cell migration gene network in C. elegans. J Cell Sci **119:** 4811-4818. https://doi.org/10.1242/jcs.03274

DELAGUE, V., A. JACQUIER, T. HAMADOUCHE, Y. POITELON, C. BAUDOT *et al.*, 2007 Mutations in FGD4 encoding the Rho GDP/GTP exchange factor FRABIN cause autosomal recessive Charcot-Marie-Tooth type 4H. Am J Hum Genet **81:** 1-16. https://doi.org/10.1086/518428

EDMONDS, M. J., and A. MORGAN, 2014 A systematic analysis of protein palmitoylation in Caenorhabditis elegans. BMC Genomics **15:** 841. https://doi.org/10.1186/1471-2164-15-841

FORMAN-RUBINSKY, R., J. D. COHEN and M. V. SUNDARAM, 2017 Lipocalins Are Required for Apical Extracellular Matrix Organization and Remodeling in Caenorhabditis elegans. Genetics **207:** 625-642. https://doi.org/10.1534/genetics.117.300207

FRIDOLFSSON, H. N., N. LY, M. MEYERZON and D. A. STARR, 2010 UNC-83 coordinates kinesin-1 and dynein activities at the nuclear envelope during nuclear migration. Dev Biol **338:** 237-250. https://doi.org/10.1016/j.ydbio.2009.12.004

FUJITA, M., D. HAWKINSON, K. V. KING, D. H. HALL, H. SAKAMOTO *et al.*, 2003 The role of the ELAV homologue EXC-7 in the development of the Caenorhabditis elegans excretory canals. Dev Biol **256:** 290-301.

GAO, J., L. ESTRADA, S. CHO, R. E. ELLIS and J. L. GORSKI, 2001 The Caenorhabditis elegans homolog of FGD1, the human Cdc42 GEF gene responsible for faciogenital dysplasia, is critical for excretory cell morphogenesis. Hum Mol Genet **10:** 3049-3062.

GILL, H. K., J. D. COHEN, J. AYALA-FIGUEROA, R. FORMAN-RUBINSKY, C. POGGIOLI *et al.*, 2016 Integrity of Narrow Epithelial Tubes in the C. elegans Excretory System Requires a Transient Luminal Matrix. PLoS Genet **12:** e1006205. https://doi.org/10.1371/journal.pgen.1006205

GÖBEL, V., P. L. BARRETT, D. H. HALL and J. T. FLEMING, 2004 Lumen morphogenesis in C. elegans requires the membrane-cytoskeleton linker erm-1. Dev Cell **6:** 865-873. https://doi.org/10.1016/j.devcel.2004.05.018

GRUSSENDORF, K. A., C. J. TREZZA, A. T. SALEM, H. AL-HASHIMI, B. C. MATTINGLY *et al.*, 2016 Facilitation of Endosomal Recycling by an IRG Protein Homolog Maintains Apical Tubule Structure in Caenorhabditis elegans. Genetics **203:** 1789-1806. https://doi.org/10.1534/genetics.116.192559

HAHN-WINDGASSEN, A., and M. R. VAN GILST, 2009 The Caenorhabditis elegans HNF4alpha Homolog, NHR-31, mediates excretory tube growth and function through coordinate regulation of the vacuolar ATPase. PLoS Genet **5:** e1000553. https://doi.org/10.1371/journal.pgen.1000553

546 HALL, D. H., 2017 Gap junctions in C. elegans: Their roles in behavior and development. Dev
547 Neurobiol **77:** 587-596. https://doi.org/10.1002/dneu.22408
548 HEDGECOCK, E. M., J. G. CULOTTI, D. H. HALL and B. D. STERN, 1987 Genetics of cell and axon
549 migrations in Caenorhabditis elegans. Development 100**:** 365-382.
550 HENCH, J., J. HENRIKSSON, A. M. ABOU-ZIED, M. LUPPERT, J. DETHLEFSEN *et al.*, 2015 The
551 Homeobox Genes of Caenorhabditis elegans and Insights into Their Spatio-Temporal
552 Expression Dynamics during Embryogenesis. PLoS One **10:** e0126947. https://doi.org/
553 10.1371/journal.pone.0126947
554 HORN, M., R. BAUMANN, J. A. PEREIRA, P. N. SIDIROPOULOS, C. SOMANDIN *et al.*, 2012 Myelin is
555 dependent on the Charcot-Marie-Tooth Type 4H disease culprit protein FRABIN/FGD4
556 in Schwann cells. Brain **135:** 3567-3583. https://doi.org/10.1093/brain/aws275
557 HULL, D., and L. TIMMONS, 2004 Methods for delivery of double-stranded RNA into
558 Caenorhabditis elegans. Methods Mol Biol **265:** 23-58. https://doi.org/10.1385/1-59259-
559 775-0:023
560 KAMATH, R. S., A. G. FRASER, Y. DONG, G. POULIN, R. DURBIN *et al.*, 2003 Systematic
561 functional analysis of the Caenorhabditis elegans genome using RNAi. Nature 421**:** 231-
562 237. https://doi.org/10.1038/nature01278
563 KHAN, L. A., H. ZHANG, N. ABRAHAM, L. SUN, J. T. FLEMING *et al.*, 2013 Intracellular lumen
564 extension requires ERM-1-dependent apical membrane expansion and AQP-8-mediated
565 flux. Nat Cell Biol **15:** 143-156. https://doi.org/10.1038/ncb2656
566 KIM, E., L. SUN, C. V. GABEL and C. FANG-YEN, 2013 Long-term imaging of Caenorhabditis
567 elegans using nanoparticle-mediated immobilization. PLoS One **8:** e53419.
568 https://doi.org/10.1371/journal.pone.0053419
569

KIPREOS, E. T., and M. PAGANO, 2000 The F-box protein family. Genome Biol 1**:** REVIEWS3002. https://doi.org/10.1186/gb-2000-1-5-reviews3002

KOLOTUEV, I., V. HYENNE, Y. SCHWAB, D. RODRIGUEZ and M. LABOUESSE, 2013 A pathway for unicellular tube extension depending on the lymphatic vessel determinant Prox1 and on osmoregulation. Nat Cell Biol **15:** 157-168. https://doi.org/10.1038/ncb2662

LANT, B., B. YU, M. GOUDREAULT, D. HOLMYARD, J. D. KNIGHT *et al.*, 2015 CCM-3/STRIPAK promotes seamless tube extension through endocytic recycling. Nat Commun **6:** 6449. https://doi.org/10.1038/ncomms7449

LIEGEOIS, S., A. BENEDETTO, J. M. GARNIER, Y. SCHWAB and M. LABOUESSE, 2006 The V0-ATPase mediates apical secretion of exosomes containing Hedgehog-related proteins in Caenorhabditis elegans. J Cell Biol **173:** 949-961. https://doi.org/10.1083/jcb.200511072

LIU, J. L., D. DESJARDINS, R. BRANICKY, L. B. AGELLON and S. HEKIMI, 2012 Mitochondrial oxidative stress alters a pathway in Caenorhabditis elegans strongly resembling that of bile acid biosynthesis and secretion in vertebrates. PLoS Genet **8:** e1002553. https://doi.org/10.1371/journal.pgen.1002553

LUBARSKY, B., and M. A. KRASNOW, 2003 Tube morphogenesis: making and shaping biological tubes. Cell **112:** 19-28. https://doi.org/10.1016/S0092-8674(02)01283-7

MAH, A. K., K. R. ARMSTRONG, D. S. CHEW, J. S. CHU, D. K. TU *et al.*, 2007 Transcriptional regulation of AQP-8, a Caenorhabditis elegans aquaporin exclusively expressed in the excretory system, by the POU homeobox transcription factor CEH-6. J Biol Chem **282:** 28074-28086. https://doi.org/10.1074/jbc.M70330520

MANCUSO, V. P., J. M. PARRY, L. STORER, C. POGGIOLI, K. C. NGUYEN *et al.*, 2012 Extracellular leucine-rich repeat proteins are required to organize the apical extracellular matrix and maintain epithelial junction integrity in C. elegans. Development **139:** 979-990. https://doi.org/10.1242/dev.075135

595 MATTINGLY, B. C., and M. BUECHNER, 2011 The FGD homologue EXC-5 regulates apical
596 trafficking in C. elegans tubules. Dev Biol **359:** 59-72.
597 https://doi.org/10.1016/j.ydbio.2011.08.011

598 MCSHEA, M. A., K. L. SCHMIDT, M. L. DUBUKE, C. E. BALDIGA, M. E. SULLENDER *et al.*, 2013
599 Abelson interactor-1 (ABI-1) interacts with MRL adaptor protein MIG-10 and is required
600 in guided cell migrations and process outgrowth in C. elegans. Dev Biol **373:** 1-13.
601 https://doi.org/10.1016/j.ydbio.2012.09.017

602 MOON, S., Y. W. LEE, W. T. KIM and W. LEE, 2014 Solution structure of CEH-37 homeodomain
603 of the nematode Caenorhabditis elegans. Biochem Biophys Res Commun **443:** 370-375.
604 https://doi.org/10.1016/j.bbrc.2013.11.13

605 MORA-LORCA, J. A., B. SAENZ-NARCISO, C. J. GAFFNEY, F. J. NARANJO-GALINDO, J. R.
606 PEDRAJAS *et al.*, 2016 Glutathione reductase gsr-1 is an essential gene required for
607 Caenorhabditis elegans early embryonic development. Free Radic Biol Med **96:** 446-461.
608 https://doi.org/10.1016/j.freeradbiomed.2016.04.017

609 NELSON, F. K., P. S. ALBERT and D. S. RIDDLE, 1983 Fine structure of the *Caenorhabditis*
610 *elegans* secretory-excretory system. Journal of Ultrastructural Research **82:** 156-171.

611 NIGAM, S. K., 2018 The SLC22 Transporter Family: A Paradigm for the Impact of Drug
612 Transporters on Metabolic Pathways, Signaling, and Disease. Annu Rev Pharmacol
613 Toxicol **58:** 663-687. https://doi.org/10.1146/annurev-pharmtox-010617-052713

614 OHNO, Y., A. KASHIO, R. OGATA, A. ISHITOMI, Y. YAMAZAKI *et al.*, 2012 Analysis of substrate
615 specificity of human DHHC protein acyltransferases using a yeast expression system.
616 Mol Biol Cell **23:** 4543-4551. https://doi.org/10.1091/mbc.E12-05-0336

617 OKA, T., T. TOYOMURA, K. HONJO, Y. WADA and M. FUTAI, 2001 Four subunit a isoforms of
618 Caenorhabditis elegans vacuolar H+-ATPase. Cell-specific expression during
619 development. J Biol Chem **276:** 33079-33085. https://doi.org/10.1074/jbc.M101652200

620 PAL, S., B. LANT, B. YU, R. TIAN, J. TONG *et al.*, 2017 CCM-3 Promotes C. elegans Germline
621 Development by Regulating Vesicle Trafficking Cytokinesis and Polarity. Curr Biol **27:**
622 868-876. https://doi.org/10.1016/j.cub.2017.02.028

623 PETER, D., R. WEBER, C. KONE, M. Y. CHUNG, L. EBERTSCH *et al.*, 2015 Mextli proteins use
624 both canonical bipartite and novel tripartite binding modes to form eIF4E complexes that
625 display differential sensitivity to 4E-BP regulation. Genes Dev **29:** 1835-1849.
626 https://doi.org/10.1101/gad.269068.115

627 PEYMEN, K., J. WATTEYNE, L. FROONINCKX, L. SCHOOFS and I. BEETS, 2014 The FMRFamide-
628 Like Peptide Family in Nematodes. Front Endocrinol (Lausanne) 5**:** 90.
629 https://doi.org/10.3389/fendo.2014.00090

630 PHORNPHUTKUL, C., Y. ANIKSTER, M. HUIZING, P. BRAUN, C. BRODIE *et al.*, 2001 The promoter
631 of a lysosomal membrane transporter gene, CTNS, binds Sp-1, shares sequences with the
632 promoter of an adjacent gene, CARKL, and causes cystinosis if mutated in a critical
633 region. Am J Hum Genet **69:** 712-721. https://doi.org/10.1086/323484

634 PRAITIS, V., E. CICCONE and J. AUSTIN, 2005 SMA-1 spectrin has essential roles in epithelial cell
635 sheet morphogenesis in C. elegans. Dev Biol **283:** 157-170.
636 https://doi.org/10.1016/j.ydbio.2005.04.002

637 QIN, L., X. LIU, Q. SUN, Z. FAN, D. XIA *et al.*, 2012 Sialin (SLC17A5) functions as a nitrate
638 transporter in the plasma membrane. Proc Natl Acad Sci U S A **109:** 13434-13439.
639 https://doi.org/10.1073/pnas.1116633109

640 SANGHAVI, P., G. LIU, A. R. VEERANAN-KARMEGAM, C. NAVARRO and G. B. GONSALVEZ, 2016
641 Multiple Roles for Egalitarian in Polarization of the Drosophila Egg Chamber. Genetics
642 **203:** 415-432. https://doi.org/10.1534/genetics.115.184622

643 SEVERSON, A. F., D. L. BAILLIE and B. BOWERMAN, 2002 A Formin Homology protein and a
644 profilin are required for cytokinesis and Arp2/3-independent assembly of cortical
645 microfilaments in C. elegans. Curr Biol **12:** 2066-2075.

646 SHAYE, D. D., and I. GREENWALD, 2015 The Disease-Associated Formin INF2/EXC-6 Organizes
647 Lumen and Cell Outgrowth during Tubulogenesis by Regulating F-Actin and
648 Microtubule Cytoskeletons. Dev Cell **32:** 743-755.
649 https://doi.org/10.1016/j.devcel.2015.01.009

650 SHAYE, D. D., and I. GREENWALD, 2016 A network of conserved formins, regulated by the
651 guanine exchange factor EXC-5 and the GTPase CDC-42, modulates tubulogenesis in
652 vivo. Development **143:** 4173-4181. https://doi.org/10.1242/dev.141861

653 SIGURBJÖRNSDÓTTIR, S., R. MATHEW and M. LEPTIN, 2014 Molecular mechanisms of de novo
654 lumen formation. Nat Rev Mol Cell Biol **15:** 665-676. https://doi.org.10.1038/nrm3871

655 SIMMER, F., M. TIJSTERMAN, S. PARRISH, S. P. KOUSHIKA, M. L. NONET *et al.*, 2002 Loss of the
656 putative RNA-directed RNA polymerase RRF-3 makes C. elegans hypersensitive to
657 RNAi. Curr Biol **12:** 1317-1319.

658 SPENCER, W. C., G. ZELLER, J. D. WATSON, S. R. HENZ, K. L. WATKINS *et al.*, 2011 A spatial
659 and temporal map of C. elegans gene expression. Genome Res **21:** 325-341.
660 https://doi.org/10.1101/gr.114595.110

661 STRAUSS, O., C. MULLER, N. REICHHART, E. R. TAMM and N. M. GOMEZ, 2014 The role of
662 bestrophin-1 in intracellular Ca(2+) signaling. Adv Exp Med Biol 801**:** 113-119.
663 https://doi.org/10.1007/978-1-4614-3209-8_15

664 SULSTON, J. E., and J. HODGKIN, 1988 Methods, pp. 587-606 in *The Nematode Caenorhabditis*
665 *elegans*, edited by W. B. WOOD. Cold Spring Harbor Press, Cold Spring Harbor, New
666 York.

667 SULSTON, J. E., E. SCHIERENBERG, J. G. WHITE and J. N. THOMSON, 1983 The embryonic cell
668 lineage of the nematode Caenorhabditis elegans. Dev Biol **100:** 64-119.
669 SUN, Q., Y. WU, S. JONUSAITE, J. M. PLEINIS, J. M. HUMPHREYS *et al.*, 2018 Intracellular
670 Chloride and Scaffold Protein Mo25 Cooperatively Regulate Transepithelial Ion
671 Transport through WNK Signaling in the Malpighian Tubule. J Am Soc Nephrol.
672 https://doi.org/10.1681/asn.2017101091
673 SUNDARAM, M. V., and M. BUECHNER, 2016 The Caenorhabditis elegans Excretory System: A
674 Model for Tubulogenesis, Cell Fate Specification, and Plasticity. Genetics **203:** 35-63.
675 https://doi.org/10.1534/genetics.116.189357
676 SUZUKI, N., M. BUECHNER, K. NISHIWAKI, D. H. HALL, H. NAKANISHI *et al.*, 2001 A putative
677 GDP-GTP exchange factor is required for development of the excretory cell in
678 Caenorhabditis elegans. EMBO Rep **2:** 530-535. https://doi.org/10.1093/embo-
679 reports/kve110
680 TIMMONS, L., and A. FIRE, 1998 Specific interference by ingested dsRNA. Nature 395**:** 854.
681 https://doi.org/10.1038/27579
682 TONG, X., and M. BUECHNER, 2008 CRIP homologues maintain apical cytoskeleton to regulate
683 tubule size in C. elegans. Dev Biol **317:** 225-233. https://doi.org/
684 10.1016/j.ydbio.2008.02.040
685 WAMELINK, M. M., E. A. STRUYS, E. E. JANSEN, E. N. LEVTCHENKO, F. S. ZIJLSTRA *et al.*, 2008
686 Sedoheptulokinase deficiency due to a 57-kb deletion in cystinosis patients causes
687 urinary accumulation of sedoheptulose: elucidation of the CARKL gene. Hum Mutat **29:**
688 532-536. https://doi.org/10.1002/humu.20685

689

690 **FIGURE LEGENDS**

691 **Figure 1. The excretory canals and induction controls.**

692 (A) Schematic diagram of the excretory canals extending over the full length of the worm with
693 basal membrane (black) and apical membrane (red) surrounding a narrow lumen (white).
694 Numbers 0-4 represent numerical assignments used to assess canal length. (B) DIC image of
695 section of posterior excretory canal of wild-type worm (N2); canal is narrow with uniform
696 diameter. Bar, 10µm. (C) Magnified DIC image of excretory canal of wild-type worm (N2).
697 Lines indicate boundaries of canal lumen/apical surface (red) and cytoplasmic/basal surface
698 (green). (D-F) Controls to ensure strong induction of dsRNA synthesis for RNAi screen, in *rrf-*
699 *3*(*pk1426*) animals expressing GFP in the canals: (D) Knockdown of cuticle collagen gene *dpy-*
700 *11*. Boxed image: Magnification of single worm. Bar = 100µm. (E) DIC and (E') GFP image of
701 *erm-1* knockdown. Bar, 10µm. (F) DIC and (F') GFP image of *exc-1* knockdown. Bar, 10µm.

702 **Figure 2. RNAi knockdowns causing formation of fluid-filled cysts or swollen lumen.**

703 (A-F) DIC images and (A'-F') GFP fluorescence of representative animals exhibiting RNAi
704 knockdown phenotypes: (A) *ceh-6*; (B) *T25C8.1* (*exc-10*); (C) *egal-1*; (D) *mop-25.2*; (E)
705 *F41E7.1* (*exc-11*); (F) *T05D4.3* (*exc-12*). Arrows: Medium and large fluid-filled cysts. All
706 bars, 10 µm.

707

708 **Figure 3. RNAi knockdowns causing periodic cytoplasmic swellings.**

709 GFP fluorescence images of swellings ("beads") along length of canals. Boxed insets of marked
710 areas are magnified to show width of lumen in regions within and between beads:. (A) *inx-12*;
711 (B) *inx-13*; (C) *ceh-37*; (D) *dhhc-2*; (E) *mxt-1*. Inset in (D) is of region posterior to end of

lumen, so lumen is not visible. Note visible vesicles in cytoplasmic beads in (D). All bars, 10 µm.

Figure 4. RNAi knockdowns causing swelling at end of lumen.

GFP fluorescence images of swollen canals at termination of lumen caused by RNAi knockdown of genes: (A) *gst-28*; (B) *gsr-1*; (C) *ceh-37*; (D) *fbxa-183*; (E) *T19D12.9* (*exc-13*); (F) *C09F12.3* (*exc-18*); (G) *best-3*; (H) *mop-235.2*; (I) *gck-3*. All images show regions of convoluted canals. Some areas in panels B, E, F, and I show additional areas that are appear as individual separated small cysts or large vesicles. Arrows: Cytoplasmic tail continuing past termination of lumen in panels B, C, G, and I. All bars, 10 µm.

Figure 5. RNAi knockdowns causing irregular basal membrane along canal length.

(A) DIC and (A') GFP fluorescence images of distal tip of canal of representative animal knocked down for *K11D12.9* (*exc-14*). Boxed areas are enlarged to right. Thin lumen indicated by black arrowheads is surrounded by area of bright GFP fluorescence. Distorted cytoplasmic shape is filled with large number of vesicles (red arrows). (B-F) GFP fluorescence of representative animals knocked down for genes: (B) *fbxa-183;* (C) *H09G03.1(exc-16)*; (D) *T08H10.1 (exc-15)*; (E) *C03G6.5 (exc-17)*; (F) *cyk-1*. Boxed areas enlarged below each panel show areas along the canals where cytoplasm surface is swollen with vesicles, and basal surface is irregular and noticeably wider than in wild-type animals. Arrows show enlarged vesicles or cysts. Bars, 10 µm.

Figure 6. Knockdown of *vha-5* leads to a wide range of phenotypes.

(A-D) GFP fluorescence of four different worms exhibiting a range of excretory canal phenotypic severity in response to *vha-5* knockdown. For each animal, the boxed area is enlarged below). (A) Periodic cytoplasmic swellings along lumen of canal. Arrows show visible lumen of normal diameter. (B) Small septate cysts in the lumen of the canal, surrounded by area of bright GFP fluorescence, and somewhat irregular diameter cytoplasm. (C) Lumen with septate cysts similar to 4B and surrounded by cytoplasm of more irregular diameter containing large cysts/vesicles. (D) Wider-diameter lumen with larger cysts, surrounded by cytoplasm filled with vesicles in a wide range of sizes. Bar, 10µm.

Figure 7. Knockdown of some *exc* genes causes tailspike defect.

DIC images of the narrow tail spike of adult hermaphrodite wild-type animal (A) and of adult mutants exhibiting RNAi knockdown for genes: (B) *F41E7.1* (*exc-11*); (d) *K11D12.9* (*exc-14*); (D) *egal-1*; (E) *mop-25.2*; (F) *inx-12*. Bars, 50µm.

Figure 8. Knockdown of two genes suppresses the Exc-5 phenotype.

(A-C) GFP fluorescence of canals in BK545 (null *exc-5*(*rh232*) mutants with RNAi-sensitized background and GFP expressed in canal cytoplasm (A) and of BK545 animals showing strong suppression when knocked down for (B) F12A10.7 (*suex-1*), or (C) C53B4.1 (*suex-2*). Exc-5 phenotype includes very short normal-diameter canals terminating in large cysts. Red arrows indicate termination of canals. Green arrows indicate areas of slight swelling of Suex canal lumen in both knockdowns. Bars, 50 µm. (D) Measurement of effect of *suex* suppression via

feeding RNAi on canal length. Canals from *exc-5* mutant and mutants with *suex* knockdown were measured according to scale in Fig. 1A. Average canal length: *exc-5*(*rh232*): 1.4, *exc-5*(*rh232*); *suex-1*(*RNAi*): 2.3, *exc-5*(*rh232*); *suex-2*(*RNAi*): 2.3. N=207 for each genotype. Analysis via 3x2 Fisher's 3x2 Exact Test (see Materials and Methods) show differences from wild-type canal length that are highly significant: P of 9.0×10^{-17} for *suex-1*, 1.7×10^{-13} for *suex-2*.

763 **Table 1.** List of strains used in this study, with genotype descriptions.

STRAIN	GENOTYPE	DESCRIPTION	REFERENCE
BK36	*unc-119(ed3)* III; *qpIs11*[*unc-119; P_{vha-1}::gfp*] I	N2 with integrated GFP marker expressed in excretory canal cytoplasm	(MATTINGLY AND BUECHNER 2011)
BK540	*rrf-3*(*pk1426*) II; *qpIs11* [*unc-119; P_{vha-1}::gfp*] I	RNAi-sensitized strain expressing GFP in canals	This study
BK541	*sid-1(pk3321)* II; *qpIs11* [*unc-119; P_{vha-1}::gfp*] I	Systemic RNAi-impaired strain expressing GFP in canals	This study
BK542	*exc-2*(*rh90*) X; *qpIs11* [*unc-119; P_{vha-1}::gfp*] I	*exc-2*(*rh90*) expressing GFP in canals	This study
BK543	*exc-3*(*rh207*) X; *qpIs11* [*unc-119; P_{vha-1}::gfp*] I	*exc-3*(*rh207*) expressing GFP in canals	This study
BK544	*exc-4*(*rh133*) *qpIs11* [*unc-119; P_{vha-1}::gfp*] I	*exc-4*(*rh133*) expressing GFP in canals	This study
BK545	*exc-5*(*rh232*) IV; *qpIs11* [*unc-119; P_{vha-1}::gfp*] I	*exc-5*(*rh232*) expressing GFP in canals	This study
BK546	*exc-7*(*rh252*) II; *qpIs11* [*unc-119; P_{vha-1}::gfp*] I	*exc-7*(*rh252*) expressing GFP in canals	This study
BK547	BK540; *exc-2*(*rh90*) X	*exc-2*(*rh90*) expressing GFP in canals in RNAi-sensitized background	This study
BK548	BK540; *exc-3*(*rh207*) X	*exc-3*(*rh207*) expressing GFP in canals in RNAi-sensitized background	This study
BK549	BK540; *exc-4*(*rh133*) I	*exc-4*(*rh133*) expressing GFP in canals in RNAi-sensitized background	This study
BK550	BK540; *exc-5*(*rh232*) IV	*exc-5*(*rh232*) expressing GFP in canals in RNAi-sensitized background	This study

764

765

766

767 **Table 2.** Genes tested exhibiting excretory canal defects via RNAi feeding ***. Genes previously found to have effects on excretory

768 canal function or development are marked with an asterisk.

Gene	Clone	Protein Class	Short Description of Known or Inferred Protein Function	Canal RNAi Phenotype	# canals examined	% mutant canals	Ave. mutant canal length
		Transcriptional and post-transcriptional factors					
*ceh-6**	K02B12.1		homeobox transcription factor	large fluid-filled cysts	Control		
*ceh-37**	C37E2.5		Otx homeobox transcription factor	periodic cytoplasmic beads	40	30%	3.3
fbxa-183	F44E7.6		F-box protein, possible effects on RNA	swollen tip with vesicles	125	66%	3.1
mxt-1	Y18D10A.8		translation regulation	cytoplasmic beads with vesicles	59	93%	2.6
		Cytoskeletal proteins and regulators					
egal-1	C10G6.1		Egalitarian exonuclease, regulates dynein	medium-sized fluid-filled cysts	40	100%	1.1
*cyk-1**	F11H8.4		*Diaphanous* formin	vesicles along swollen cytoplasm	77	77%	3.1
		Transporters, channels, and receptors					
*inx-12**	ZK770.3		innexin gap junction protein	periodic cytoplasmic beads	46	96%	2.7
*inx-13**	Y8G1A.2		innexin gap junction protein	periodic cytoplasmic beads	50	80%	2.8
*vha-5**	F35H10.4		vacuolar ATPase component	beads, vesicles, swollen cytoplasm	78	59%	2.5
best-3	C01B12.3		bestrophin chloride channel	Swollen luminal tip	36	28%	3.4
exc-11	F41E7.1		Na^+/H^+ solute carrier (SLC9 family)	medium-sized fluid-filled cysts	34	97%	1.7
exc-13	T19D12.9		sialic acid solute carrier (SLC17 family)	swollen tip, vesicles, convolutions	23	22%	3.3
exc-18	C09F12.3		Nematode 7tm GPCR	vesicles along swollen cytoplasm	40	13%	3.1
		Vesicle movement regulators					
*gck-3**	Y59A8B.23		germinal center kinase protein	swollen tip, vesicles, convolutions	76	57%	3.5
mop-25.2	Y53C12A.4		scaffolding for endocytic recycling	medium-sized fluid-filled cysts, vesicles along swollen cytoplasm	20	100%	1.1
		Enzymatic activities					
dhhc-2	Y47H9C.2		Zn-finger, palmitoyltransferase	cytoplasmic beads with vesicles	57	21%	3.5
gsr-1	C46F11.2		glutathione reductase	swollen tip, vesicles, convolutions	73	5%	3.4

gst-28	Y53F4B.31	glutathione-S-transferase, prostaglandin isomerase	swollen tip with vesicles	26	27%	3.4
exc-10	T25C8.1	sedoheptulose kinase	large fluid-filled cysts	63	68%	3.3
exc-14	K11D12.9	RING finger, possible E3 ubiquitin ligase	vesicles along swollen cytoplasm	36	100%	1.4
exc-15	T08H10.1	aldo-keto reductase	vesicles along swollen cytoplasm	27	15%	3.4
		Unknown function				
exc-12	T05D4.3	Nematode-only transmembrane protein	medium-sized fluid-filled cysts	53	79%	2.6
exc-16	H09G03.1	*Caenorhabditis*-only protein	vesicles along swollen cytoplasm	134	7%	3.3
exc-17	C03G6.5	Nematode conserved-domain protein	vesicles along swollen cytoplasm	54	20%	3.5
		Suppressors of *exc-5* mutation				
suex-1	F12A10.7	unknown *Caenorhabditis* protein	suppresses *exc-5* mutant cysts			
suex-2	C53B4.1	solute carrier (SLC22 family)	suppresses *exc-5* mutant cysts			

769

Fig. 1

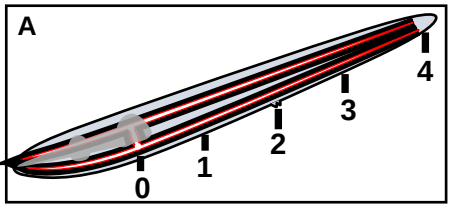

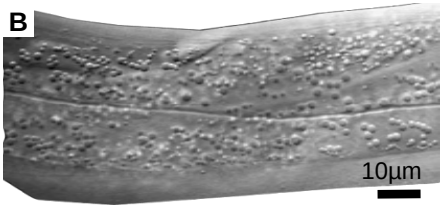

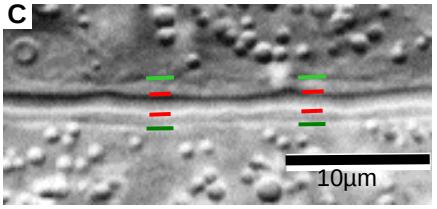

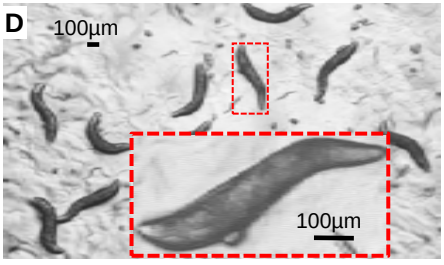

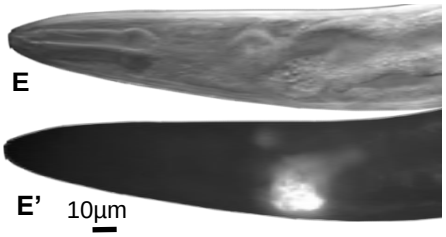

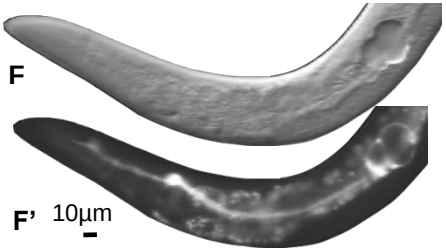

Fig. 2

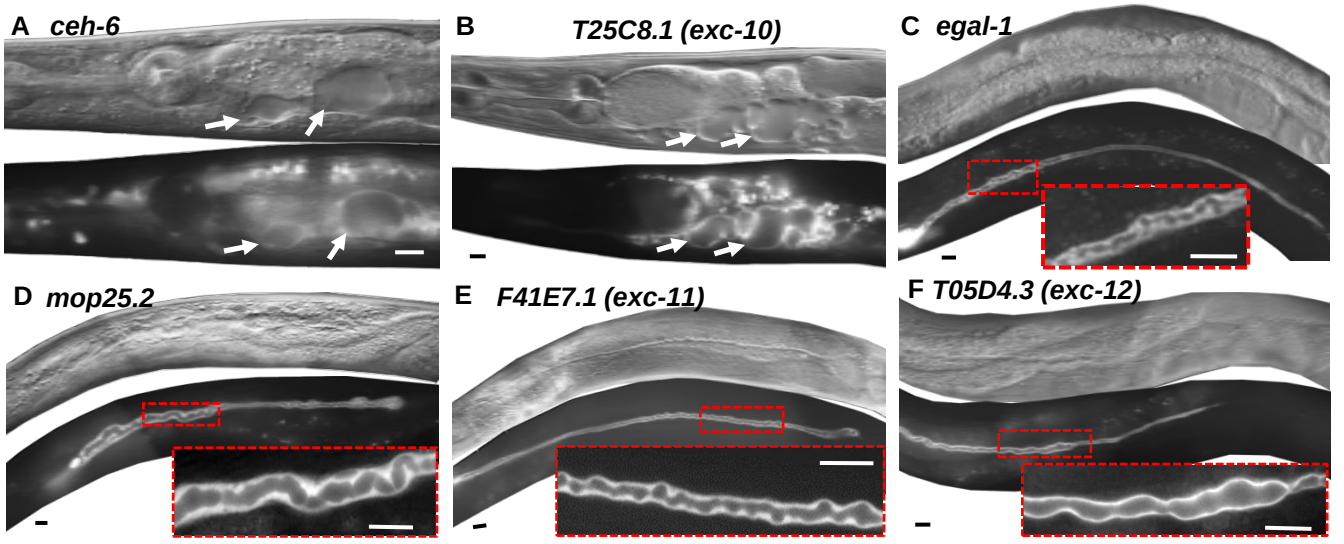
A ceh-6
B T25C8.1 (exc-10)
C egal-1
D mop25.2
E F41E7.1 (exc-11)
F T05D4.3 (exc-12)

Fig. 3

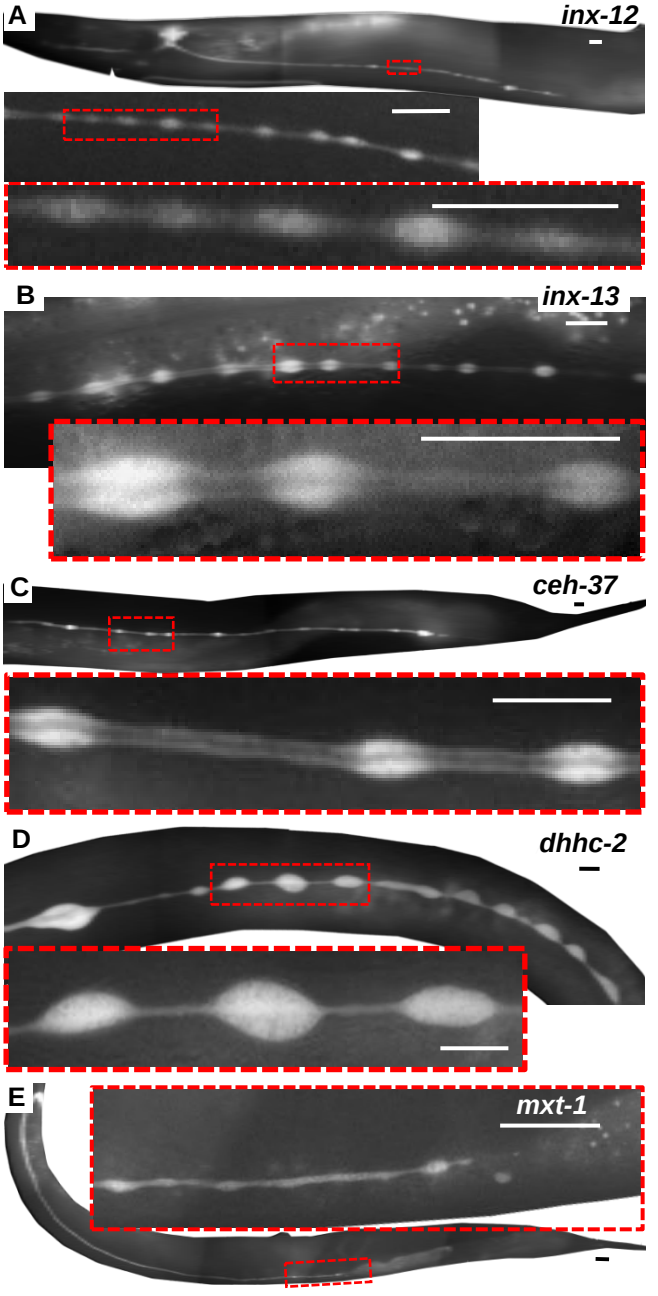

Fig. 4

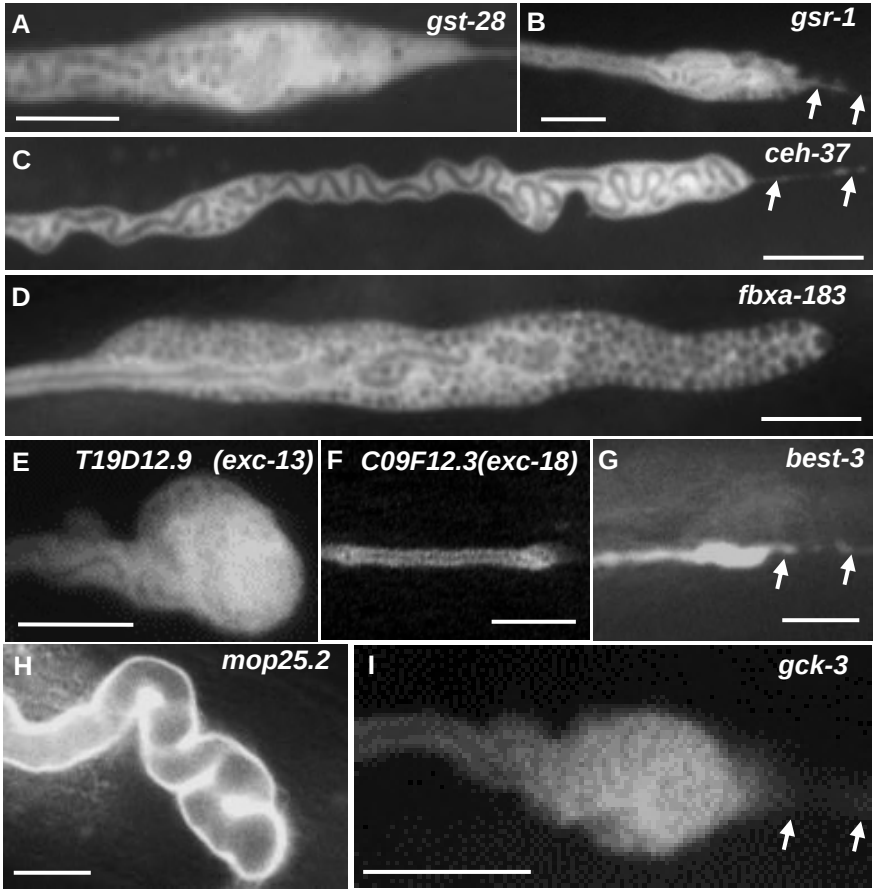
A
gst-28
B
gsr-1
C
ceh-37
D
fbxa-183
E
T19D12.9 (exc-13)
F
C09F12.3(exc-18)
G
best-3
H
mop25.2
I
gck-3

Fig. 5

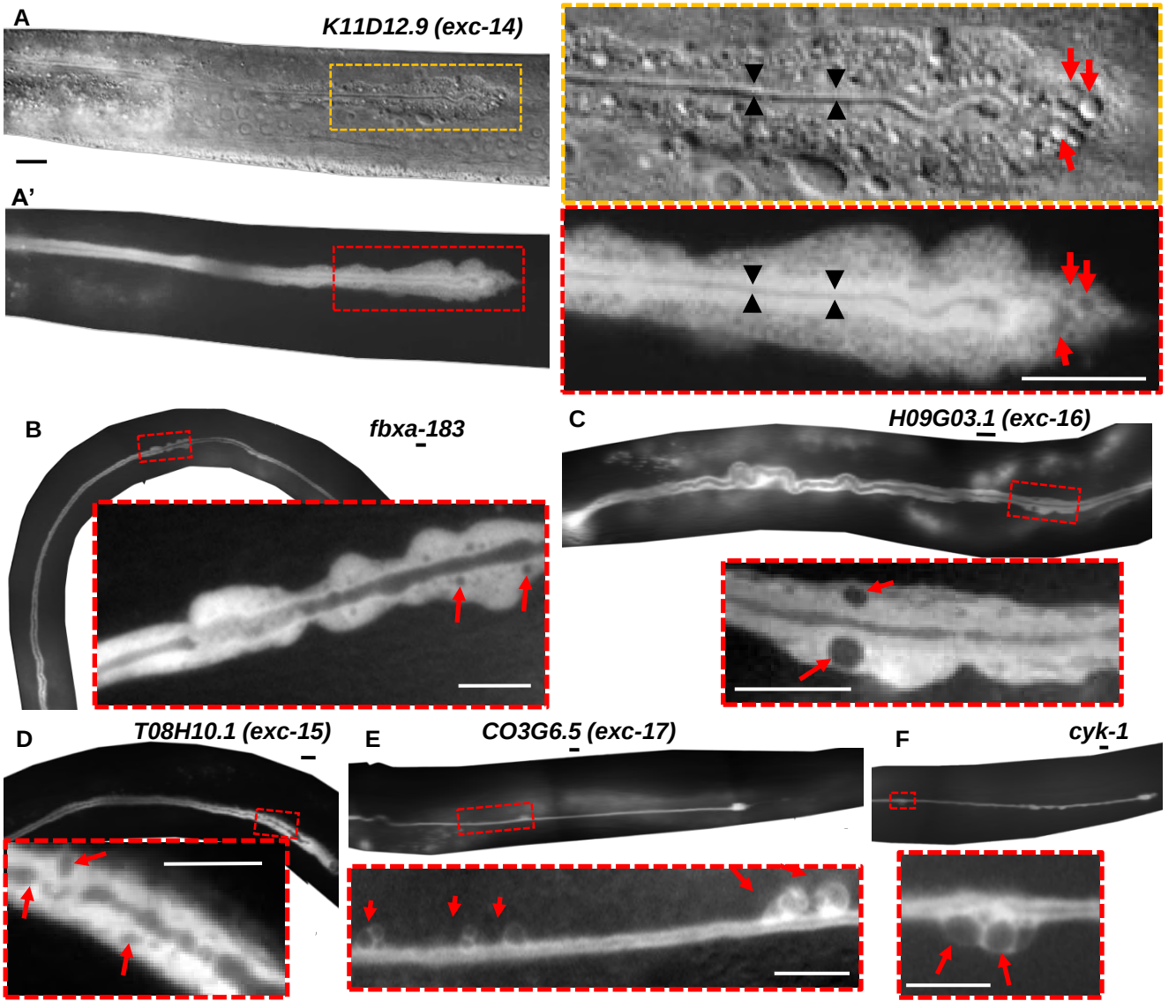
A
K11D12.9 (exc-14)
A'
B
fbxa-183
C
H09G03.1 (exc-16)
D
T08H10.1 (exc-15)
E
CO3G6.5 (exc-17)
F
cyk-1

Fig. 6

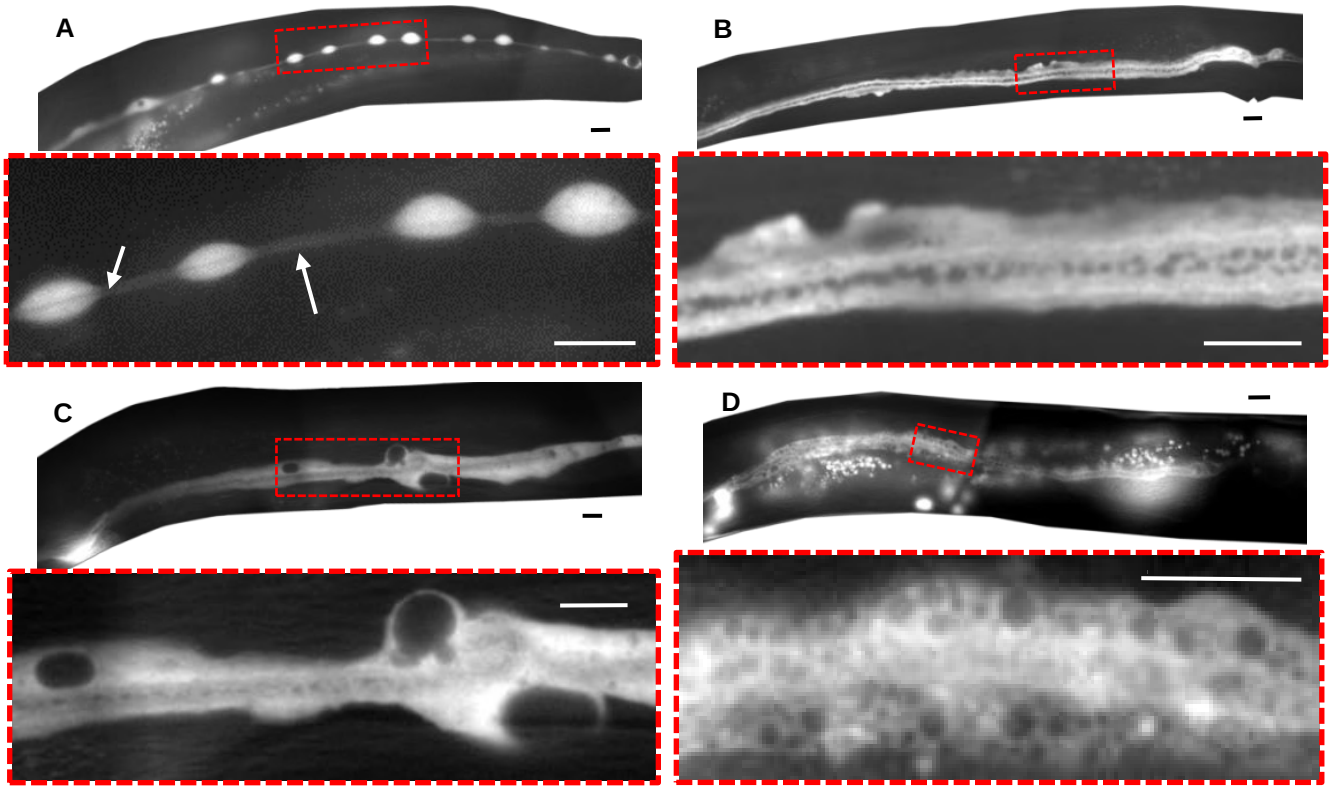

Fig. 7

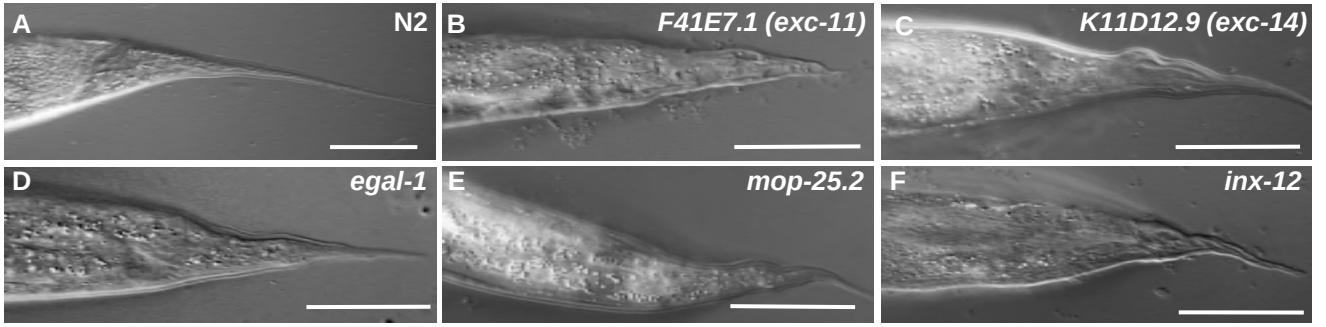

Fig. 8

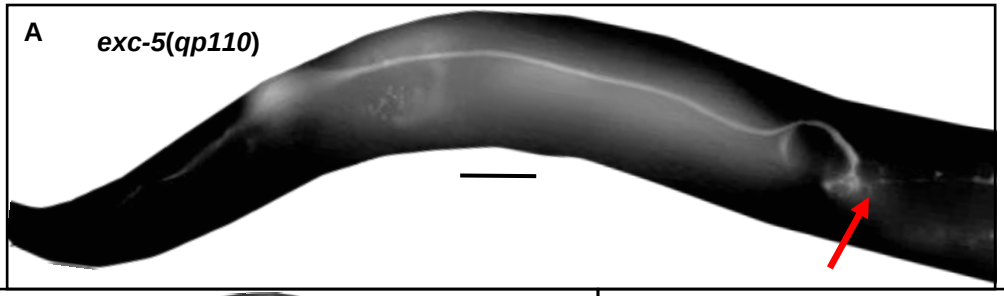
A
exc-5(qp110)

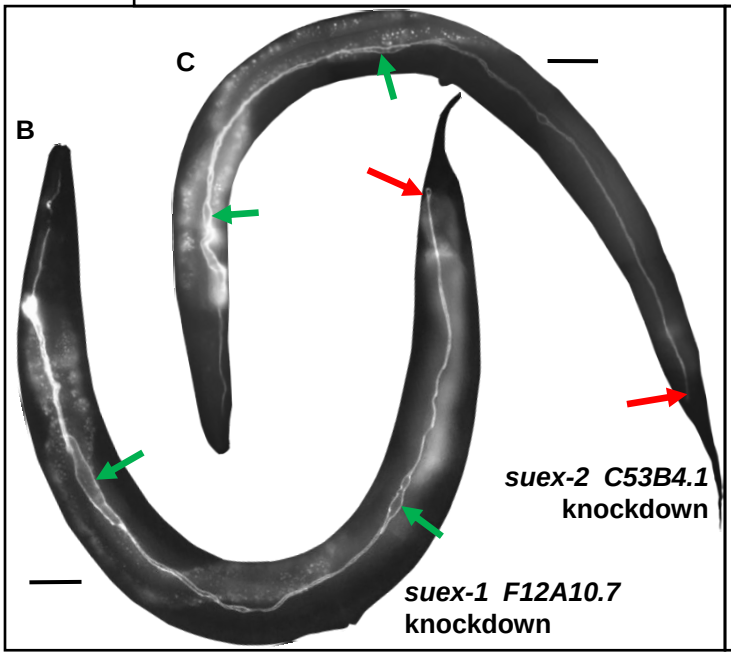
B
C
suex-2 C53B4.1
knockdown
suex-1 F12A10.7
knockdown

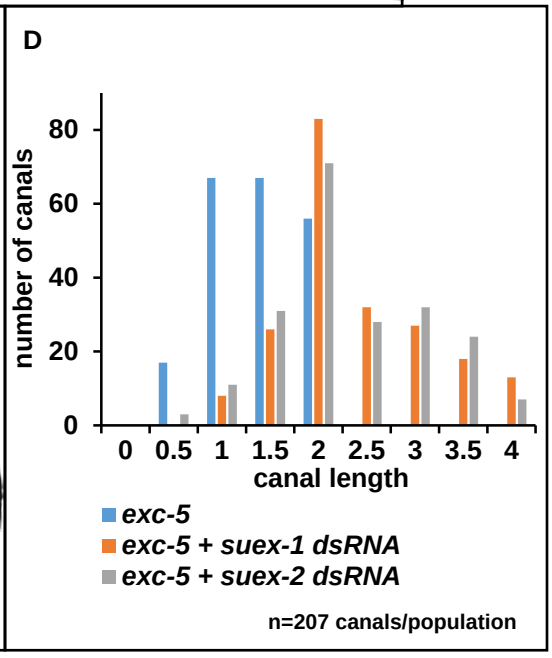
D
number of canals
0
20
40
60
80
0
0.5
1
1.5
2
2.5
3
3.5
4
canal length
exc-5
exc-5 + suex-1 dsRNA
exc-5 + suex-2 dsRNA
n=207 canals/population